



This is a repository copy of *The effects of friction management materials on rail with pre-existing RCF surface damage*.

White Rose Research Online URL for this paper:

<https://eprints.whiterose.ac.uk/115524/>

Version: Accepted Version

Article:

Harwick, C., Lewis, R. and Stock, R. (2017) The effects of friction management materials on rail with pre-existing RCF surface damage. *Wear*, 384-385. pp. 50-60. ISSN 0043-1648

<https://doi.org/10.1016/j.wear.2017.04.016>

Article available under the terms of the CC-BY-NC-ND licence
(<https://creativecommons.org/licenses/by-nc-nd/4.0/>)

Reuse

This article is distributed under the terms of the Creative Commons Attribution-NonCommercial-NoDerivs (CC BY-NC-ND) licence. This licence only allows you to download this work and share it with others as long as you credit the authors, but you can't change the article in any way or use it commercially. More information and the full terms of the licence here: <https://creativecommons.org/licenses/>

Takedown

If you consider content in White Rose Research Online to be in breach of UK law, please notify us by emailing eprints@whiterose.ac.uk including the URL of the record and the reason for the withdrawal request.



eprints@whiterose.ac.uk
<https://eprints.whiterose.ac.uk/>

THE EFFECTS OF FRICTION MANAGEMENT MATERIALS ON RAIL WITH PRE EXISTING RCF SURFACE DAMAGE

Dr. C. Hardwick¹, Prof. R. Lewis², Dr. R. Stock³

¹L.B. Foster Rail Technologies U.K. Ltd, ²The University of Sheffield, ³L.B. Foster Rail Technologies Corp

United Kingdom

United Kingdom

BC. Canada

Corresponding Author: CHardwick@LBFoster.com

Abstract

Management of rolling contact fatigue (RCF) risk is a critical maintenance activity in railway operations. Practical means of RCF mitigation involve: 1) preventative and corrective grinding to remove RCF cracks; 2) management of wheel and rail profiles to minimize peak contact pressures; and 3) selection of appropriate rail metallurgy. In addition, reduction of traction forces by application of dry film Top of Rail friction modifiers (FM) has recently been shown to reduce crack growth and extend grinding intervals.

Hydro-pressurisation and crack face lubrication are processes by which liquid materials (e.g., water), enter pre-existing RCF cracks and under wheel/rail contact pressure and cause accelerated crack growth, leading to spalling and shelling on rail and wheels. Thus, any liquid material added deliberately to the wheel/rail interface should be considered carefully in terms of the potential for aggravating RCF damage. This study compares the impact on hydro-pressurization and crack face lubrication of different types of materials designed for application to the top of rail using twin disc testing. One type of FM material is water-based, drying providing solid particles to the rail-wheel contact. Two other types are oil or oil-plus-water-based (hybrid material) that do not naturally dry and have been introduced more recently to the market. In addition, a commonly used gauge face lubricant (grease) was evaluated.

Keywords: RCF, Friction Modifier, Lubrication, Hydro-pressurisation

1 INTRODUCTION

Management of Rolling Contact Fatigue (RCF) is associated with high capital spending for all railway operators globally. The key motivation for managing RCF is related to extending rail life and associated with overcoming safety risks like rail breakages. Successful mitigation strategies include a combination of selecting the appropriate RCF resistant rail grade, applying a preventive (if necessary also corrective) maintenance strategy including optimised wheel and rail profiles and introducing a friction management program [1]. The term friction management refers to a combined application of gauge face (GF) lubrication and top of rail (TOR) friction control. Numerous studies into the cause and effect of RCF have been carried out over the years, however, only a limited number have investigated the impact of friction management on RCF development [2].

RCF development is related to high tangential forces transmitted between two bodies (wheel and rail) in rolling/sliding contact. These tangential forces can be attributed to creepage between wheel and rail due to curving, hunting and/or profile mismatch. Generally, the vertical loads and the friction levels between wheel and rail are major contributors to the development of these tangential forces. Besides, tangential forces mainly in longitudinal rail direction are also related to braking and acceleration forces transmitted by vehicle wheels. In all cases rail and/or wheel will develop RCF if the material cannot withstand these forces. RCF development can be divided in two phases: the first phase includes plastic material flow as a response to these tangential forces and the initiation of first cracks. For this phase, different models like the Shakedown limit or the DangVang criterion [3, 4] are applied to describe the material and damage behaviour. The second phase is related to crack growth of these initiated cracks until a critical failure of the component is happening. Multiple crack growth criteria have been developed and commonly used over the years to describe this RCF development phase.

RCF damage will mainly manifest in the form of cracks on the rail surface. The most common type of RCF are so called Head Check cracks or also referred to as GCC (gauge corner cracking) as these periodic cracks typically form at the gauge corner (GC) of high rails in curves [5]. Besides Head Checks, cracks or whole crack networks can also form on the running surface of the low and/or the high rail in curves or sometimes even in tangent track [6]. Additionally, there is ongoing debate if surface defects called squats and/or studs can be classified as an RCF defect [8]. The growth behaviour of these RCF surface cracks can be divided into two classes: after growing some few mm into the rail material cracks can branch upwards, coalesce with neighbouring cracks and then result in material breaking out of the rail surface (spalling). In the more dangerous case these cracks can turn downwards, continue to grow into the rail head and will finally result in a rail break.

There are a number of Friction Management materials (e.g., greases, oils, Friction Modifiers, hybrids) available that can be applied to the rail wheel contact [8]. Some of these materials have shown in previous studies to prevent the onset of RCF formation when applied to an unworn/undamaged rail surface [2]. This study will examine the interaction of selected Friction Management materials with pre-initiated RCF damage on rail material.

2 EXPERIMENTAL DETAILS

2.1 Test Apparatus and Specimens

Twin-disc testing has been performed using R8T wheel material (2.6GPa hardness and 860-980 MPa tensile strength) and R350HT grade rail (3.4GPa hardness and ≥ 1175 MPa tensile strength). These materials were chosen as R8T is a very common wheel material in Europe and R350HT is seeing more frequent use as it has improved wear and RCF resistance over standard grate rail. R350HT is also used in heavy haul. Discs were run together under realistic contact pressure and slip conditions (in the possible spread for a top of rail/wheel tread contact or gauge corner/wheel flange contact for a UK passenger train and top of rail/wheel tread for heavy haul) for a predefined number of cycles to generate surface damage prior to the application of the product. Contact conditions were maintained for a further predefined duration and product was applied prior to performance assessment by means of both surface and subsurface specimen analysis and assessment of mass loss and frictional characteristics.

Materials assessed included water, as a baseline, a gauge face lubricant and several TOR treatments.

With the wider acceptance of the FM concept and taking into account recent material developments, the available products can be classified into three groups with respect to their general type:

- TOR Friction Modifiers (water-based drying material)
- TOR Lubricants (non-drying materials, oil or grease based)
- TOR Hybrid Materials (lubricant type, oil in water suspension, non-drying material)

Materials from all the above mentioned categories were assessed, including both synthetic oil-based (low viscosity) and grease-based (high viscosity) TOR lubricants. This paper defines a water based material to have a water content of at least 50% or more. A more detailed classification and characterisation of tested TOR materials is available in [8].

Twin disc testing was carried out using the Sheffield University Rolling Sliding machine (SUROS), as shown in Figure 1. Details of the machine usage and capabilities have been described previously [9].

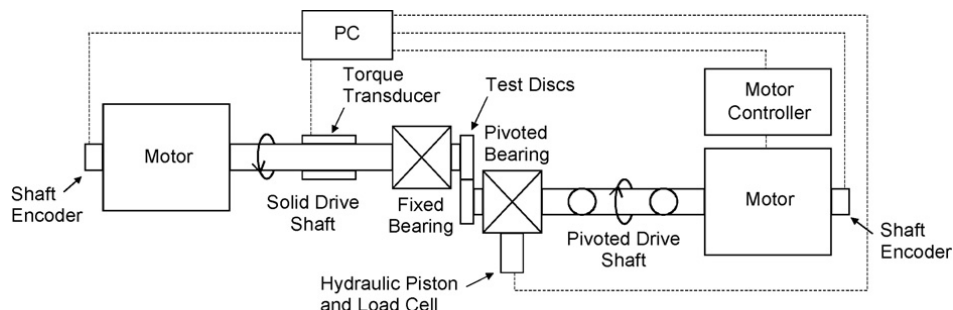


Figure 1 : SUROS twin disc machine (Schematic)

The machine is based on a Colchester Mascot lathe with an independently driven AC motor at the tailstock end. Shaft encoders continually monitor the rotational speed. A torque

transducer mounted on one of the shafts continually monitors the torque (**uncertainty $\pm 1.25\%$**). The specimen discs are hydraulically loaded together and driven at controlled speeds by the independent motors. A load cell mounted beneath the hydraulic jack ensures that the required load is continually applied Slip levels are achieved by alteration of the rotational speed of the AC motor. Data acquisition is performed by a desktop computer. This is also used to control load and slip parameters. The wheel disc acts as the driving disc and the rail disc acts as the brake.

Specimens used during the testing were cylindrical and were cut from R8T wheel rims and R350HT grade rail sections. They were machined to a diameter of 47 mm with a contact track width of 10 mm. The contact surfaces were ground to achieve an average roughness of $1 \mu\text{m}$, **which is typical of worn in wheels and rails [10]**.

2.2 Test Conditions

Tests were carried out with the wheel disc driving and the rail disc braking, this simulates an accelerating wheelset. A nominal speed of 400 rpm (1 m/s surface speed), average maximum contact pressure of 1500 MPa and 1% creep was used for all tests. These test conditions are typical of previous twin-disc studies on RCF [9, 11, 12]. Testing was carried out in two phases, first establishing baseline measurements and second evaluating the effects of the products.

Testing performed as part of the INNOTRACK project [13] showed, that when using a premium rail up to 4000 dry cycles were required to reach the stage at which water application resulted in accelerated crack growth. Specimens were run under dry conditions initially for 4000 cycles and then for a further 21000 cycles with the application of a product. It was decided to test for a defined number of cycles as opposed to propagating cracks to a given depth and using, for example, an eddy current crack detection system, to determine when this is reached. This approach was preferred as it allows for the effect of the product application to be compared directly with respect to crack frequency, length, depth and orientation rather than just the RCF life. Full test details are shown in Table 1.

Table 1: Experimental Matrix

Test	Product	Notes	Dry Cycles	Product Cycles
1	n/a	Initial Dry	4000	0
2	n/a	Full Cycles	25000	0
3	Water	Wet Rail Baseline	4000	21000
4	A	TOR FM (Drying)	4000	21000
5	B	Gauge Face Lubricant	4000	21000
6	C	TOR Lubricant (Low Viscosity Oil)	4000	21000
7	D	TOR Lubricant (High Viscosity Grease)	4000	21000
8	E	TOR Hybrid (Non Drying)	4000	21000

2.3 Baseline Measurement

As indicated in Table 1, baseline measurements were established under dry (absence of product) conditions for both 4000, and 25000 cycles. This allows for the assessment of damage prior to the application of a product and an assessment of the total damage accumulation over the full test duration in the absence of a product. As it is a standard for RCF studies [12], water was used as the control material.

2.4 Product Application

Prior to product application, wheel and rail specimens were subjected to 4000 cycles to accumulate surface fatigue. Products were applied in accordance with the Network Rail standard for lubricant assessment [14]. Top of rail products were applied at a rate of 0.05g / 500 cycles using a small brush / cotton swab, water was dripped into the contact at 1 drip / s through a top mount burette.

It must be recognised that this paper focuses on the influence of the friction management materials, for that reason the application rate is kept constant for all products.

3 RESULTS

3.1 Traction Coefficient Data

The frictional force between the specimens was recorded for the duration of all tests. Traction data plots are shown in Figure 2 – 8. The periods of dry cycles and product application are identified on the plots.

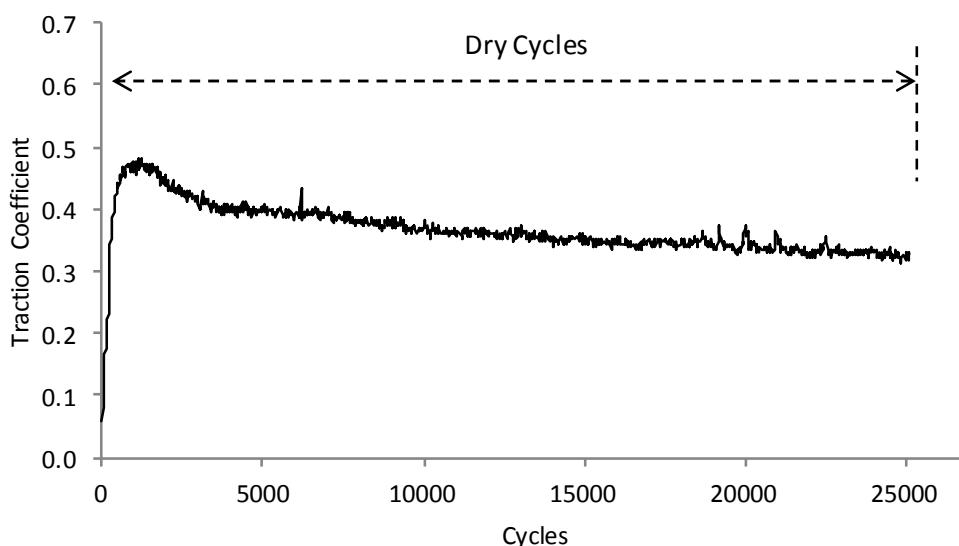


Figure 2: Traction Coefficient Dry (1500MPa, 1% Creep, 400 rpm)

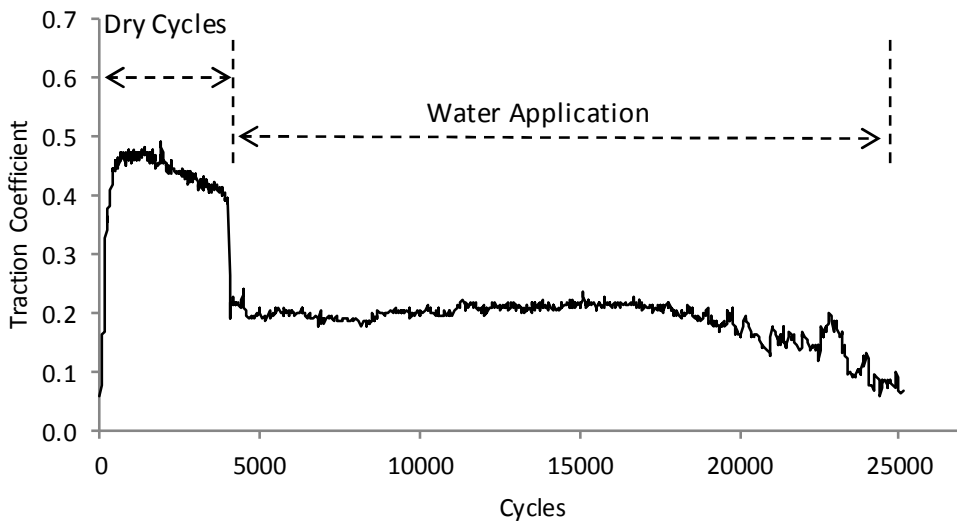


Figure 3: Traction Coefficient Water (1500MPa, 1% Creep, 400 rpm)

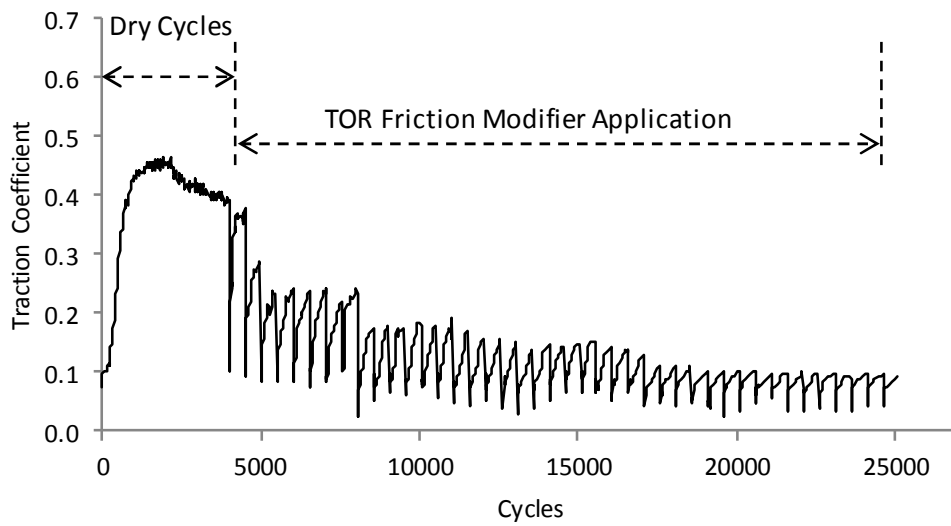


Figure 4: Traction Coefficient TOR FM (1500MPa, 1% Creep, 400 rpm)

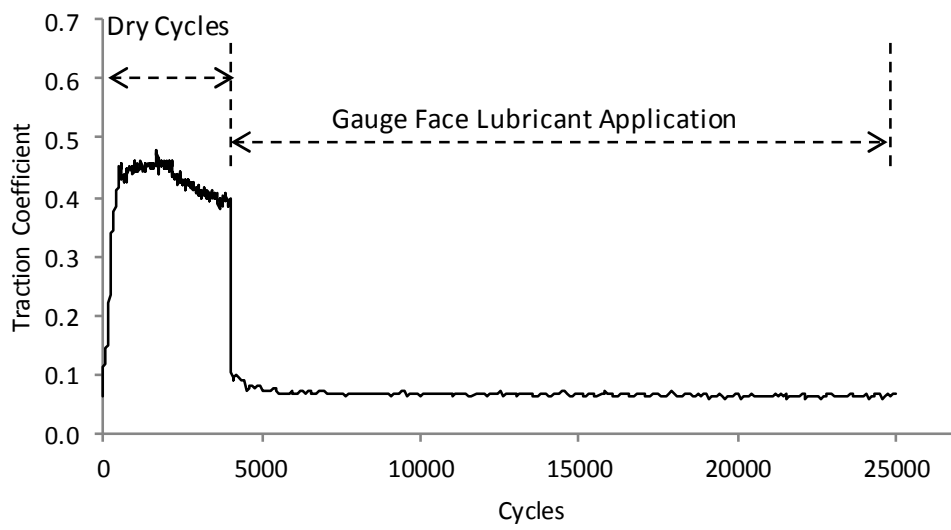


Figure 5: Traction Coefficient GF Lubricant (1500MPa, 1% Creep, 400 rpm)

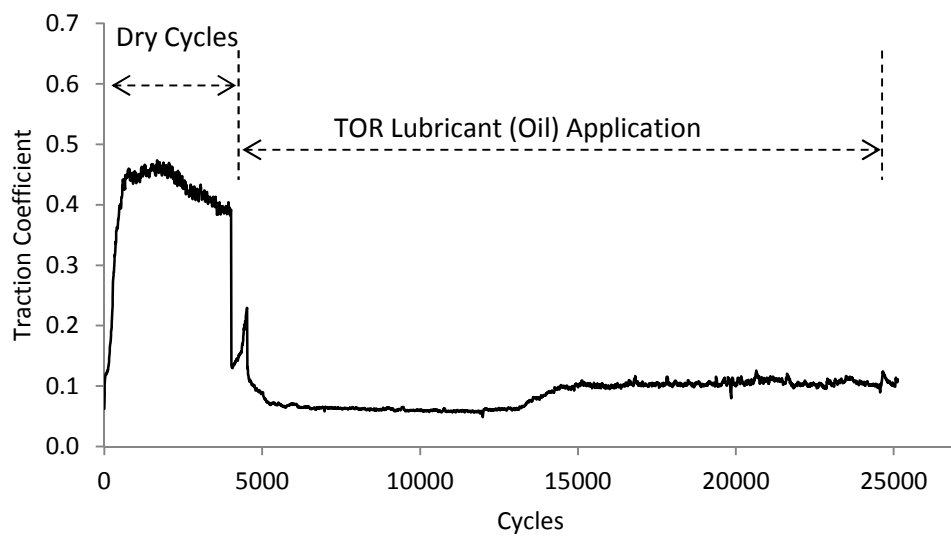


Figure 6: Traction Coefficient TOR Lubricant (Oil) (1500MPa, 1% Creep, 400 rpm)

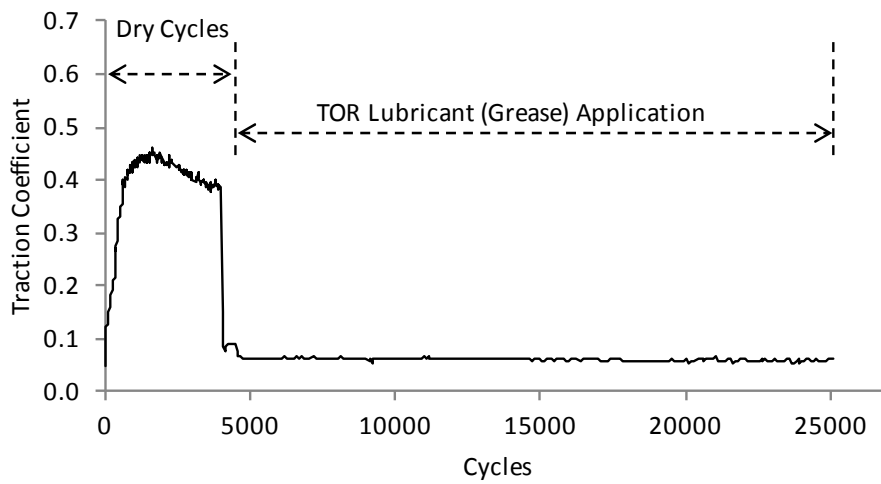


Figure 7: Traction Coefficient TOR Lubricant (Grease) (1500MPa, 1% Creep, 400 rpm)

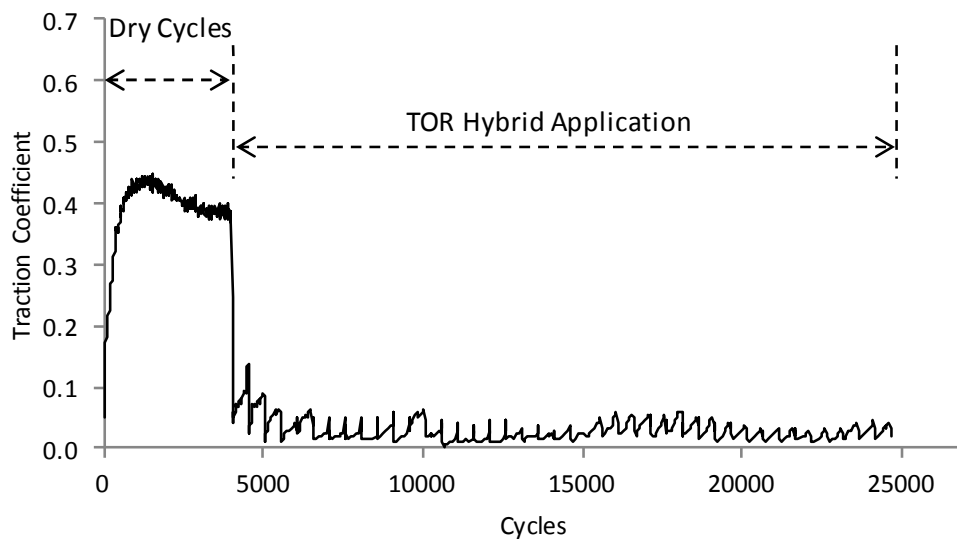


Figure 8: Traction Coefficient TOR Hybrid (1500MPa, 1% Creep, 400 rpm)

During product application, the value for traction coefficient (see

Table 2) was determined by the average traction coefficient between 8000 and 15000 cycles, this disregards the influence of the initial 4000 dry cycles and allows for traction stabilisation under product application.

Table 2: Average Traction Coefficient Data

Test	Product	Notes	Avg. CoT
1	n/a	Initial Dry	0.40
2	n/a	Full Cycles	0.36
3	Water	Wet Rail Baseline	0.2
4	A	TOR FM (Drying)	0.12
5	B	Gauge Face Lubricant	0.07
6	C	TOR Lubricant (Oil)	0.07
7	D	TOR Lubricant (Grease)	0.06
8	E	TOR Hybrid (Non Drying)	0.02

3.2 Rail Wear Data

Wear rate of the rail material was determined through pre and post-test measurement of mass. Specimens were cleaned with a solvent prior to measurement to remove traces of the applied product. Wear rate is presented as $\mu\text{g}/\text{cycle}$ (see Figure 9).

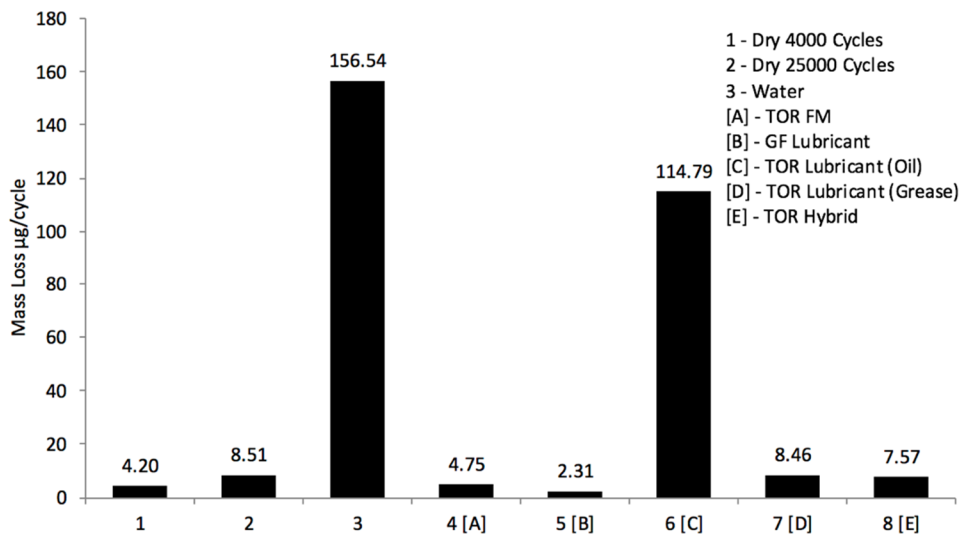


Figure 9: Rail Wear Rate Data

The percentage change in wear relative to dry contact conditions (Test 2) are detailed in Table 3. N.B. Positive values indicate an increase in wear; negative values correspond to a reduction.

Table 3: Wear Rate (Percentage Change vs Baseline)

Test	Product	Notes	% Change
1	n/a	Initial Dry	n/a
2	n/a	Full Cycles	n/a
3	Water	Wet Rail Baseline	1739.10
4	A	TOR FM (Drying)	-44.17
5	B	Gauge Face Lubricant	-72.84
6	C	TOR Lubricant (Oil)	1248.54
7	D	TOR Lubricant (Grease)	-0.61
8	E	TOR Hybrid (Non Drying)	-11.04

3.3 Surface and Subsurface Crack Analysis

Post testing, the rail specimens were cleaned with a solvent in an ultrasonic bath to remove any residual product. Surface images were then taken. For subsurface crack analysis, specimens were sectioned at the area exhibiting the most severe damage. Specimens were then mounted and polished and examined under a microscope. Crack length, depth and orientation were characterised and photographed.

In the following section, the surface of the rail specimen will be first be characterised followed by analysis of subsurface crack formations.

An overview of the specimen rolling surfaces is shown in Figure 10.

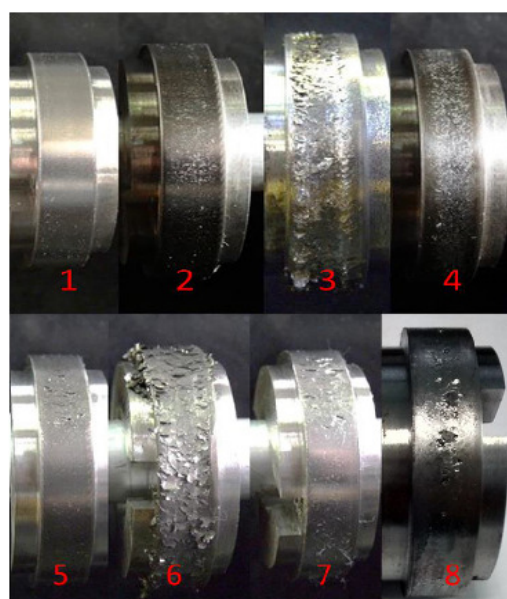


Figure 10: Surface Images for Test Samples 1 - 8

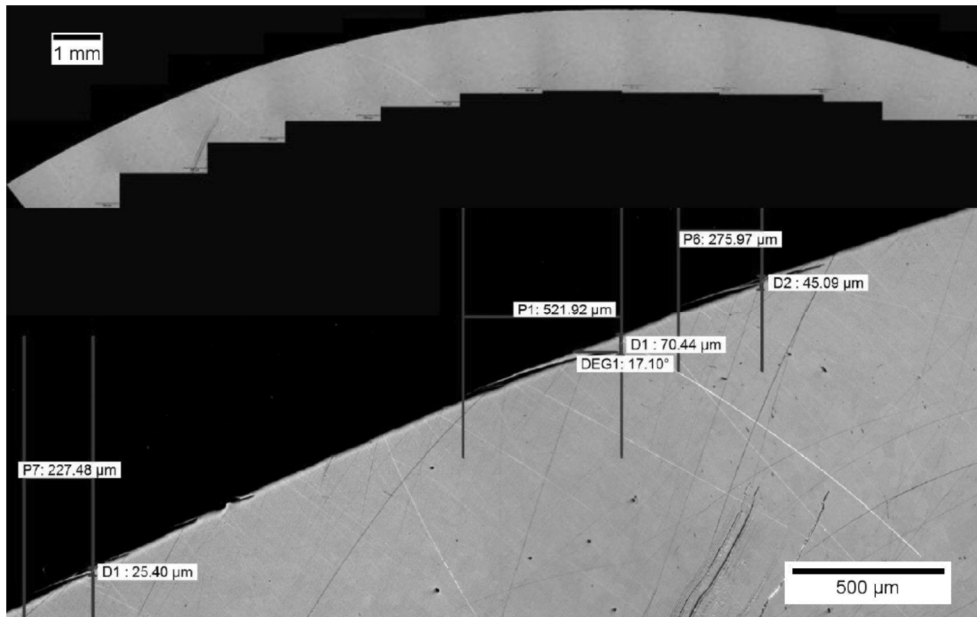


Figure 11: Test 1, Initial Dry, 4000 Cycles

The surface of the R350HT rail specimen (see Figure 10 Sample 1) shows minimal signs of damage after 4000 dry cycles, it does appear rougher than a new disc, however, there are no signs of large surface cracking and no spalling is present on the surface. Looking at the subsurface (see Figure 11) the overview is very smooth with no cracks visible. Closer inspection highlighted a few very shallow surface breaking cracks with lengths ranging from 227μm - 522μm and depth ranging from 25μm - 70.44μm. The crack angle was very shallow running along the surface with slight turning at the crack tip with a maximum angle of 17 degrees.

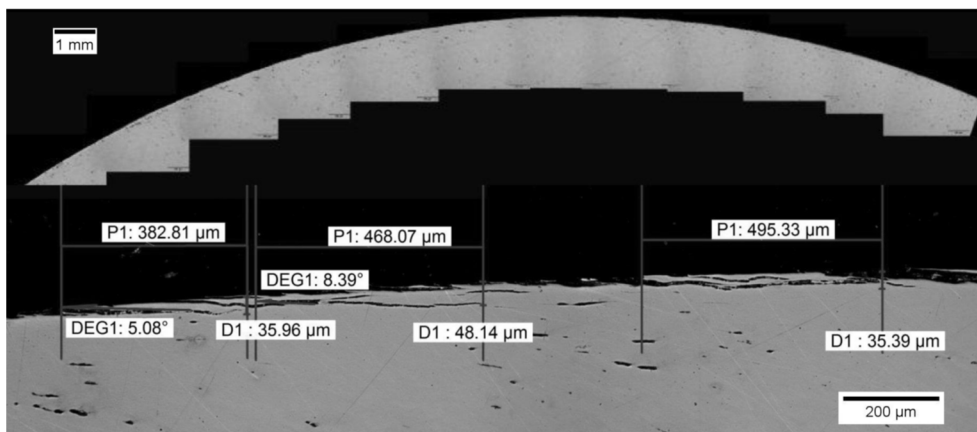


Figure 12: Test 2, Dry Baseline, 25000 Cycles

The rail specimen surface (see Figure 10 Sample 2) displayed increased surface damage after 25000 dry cycles, there are signs of surface cracking, but no signs of spalling. Looking at the subsurface (see Figure 12) the overview is very smooth with no large cracks visible. Closer inspection highlighted frequent very shallow surface breaking cracks running parallel to the

surface and numerous subsurface cracks. Signs of wear by delamination can be seen. Crack length ranges from 383 μm - 495 μm and depth ranges from 35 μm - 48 μm . The crack angle was very shallow running along the surface a maximum angle of 8 degrees.

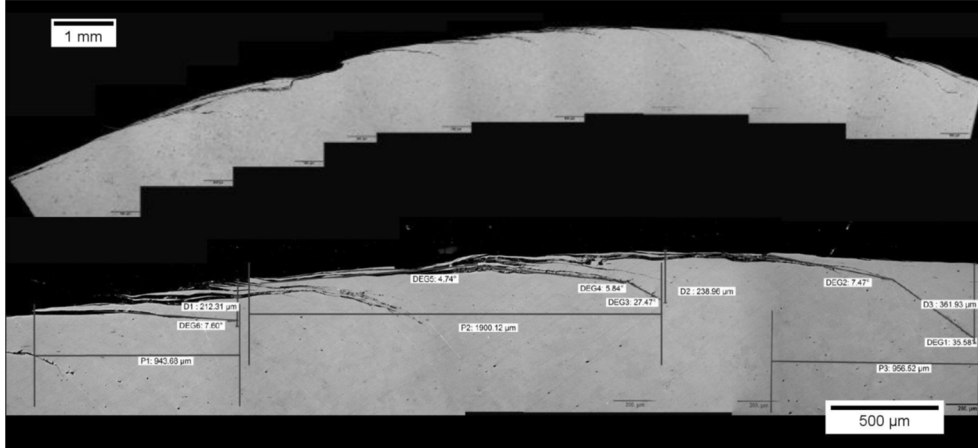


Figure 13: Test 3, 4000 Cycles Dry, 21000 Cycles Water

With water applied to the rail specimen for 21000 cycles after 4000 initial dry cycles, severe damage is visible on the surface (see Figure 10 Sample 3). There is large scale flaking and delamination of the surface material. Sites of spalling are also present.

Looking at the subsurface (see Figure 13) the overview shows multiple surface breaking cracks running parallel to the surface and then turning down into the material. There is also an area where a large chunk of material has been removed in the form of a spall. Crack length has increased over the dry running case (see Figure 12). Crack length ranges from 944 μm - 1900 μm and depth ranges from 212 μm - 361 μm . The crack angle starts very shallow running along the surface, but then turns down to angles of 36 degrees with some cracks almost vertical.

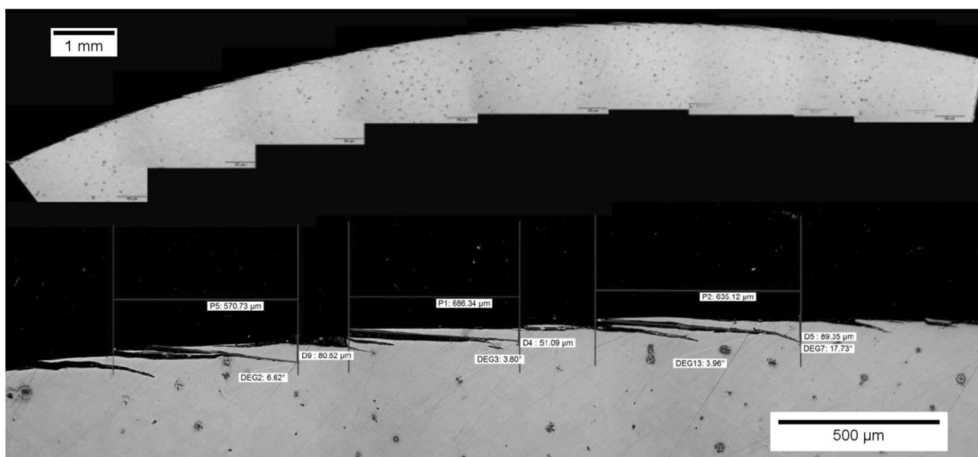


Figure 14: Test 4, 4000 Cycles Dry, 21000 Cycles TOR FM

With the application of the water based TOR FM for 21000 cycles after 4000 dry cycles, the surface of the rail disc (see Figure 10 Sample 4) exhibits little sign of damage and is very similar in appearance to the dry baseline case (Test 2). There are no visible surface cracks, however, signs of frequent short and shallow surface breaking cracks are visible under magnification (see Figure 14). The crack length ranges from 570µm - 686µm, with depth ranging from 51µm - 90µm. The crack angle is very shallow running along the surface with a maximum angle of 18 degrees. This is the only tested product that did dry on the disk surface between the application cycles.

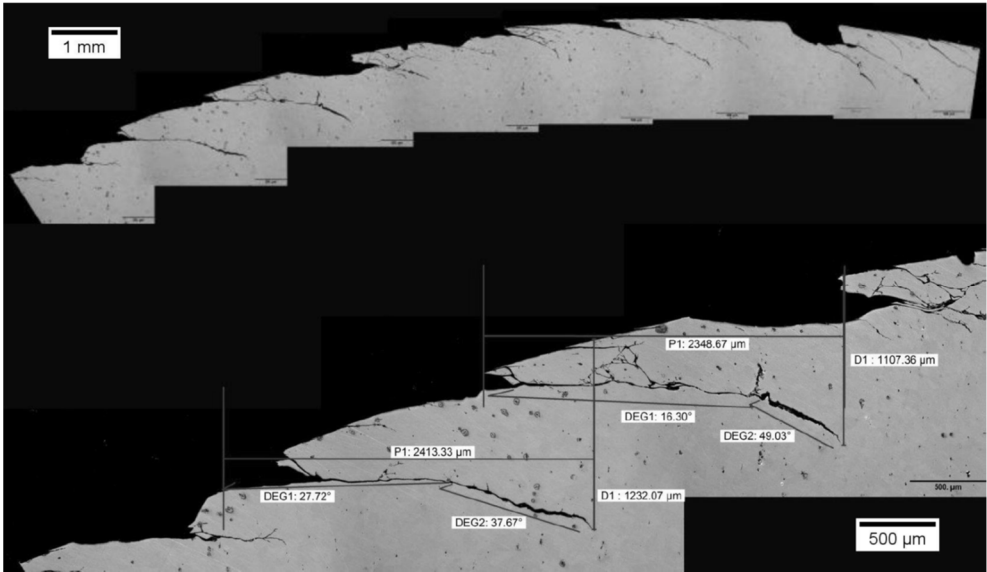


Figure 15: Test 5, 4000 Cycles Dry, 21000 Cycles GF Lubricant

The application of a gauge face lubricant is such that the surface of the specimen (see Figure 10 Sample 5) exhibits localized spalling and surface breaking cracks alongside regions of minimal surface damage. The cross-section (taken at a spalling region) depicts long cracks which penetrate deep into the rail material. Several cracks can be seen to bifurcate towards the surface which will lead to spalling, large areas of material loss can also be observed. Cracks were generally long ranging from 2350 µm - 2415 µm and reaching depths of 1100 µm - 1232 µm. The crack angle varied from 49 to almost 90 degrees.

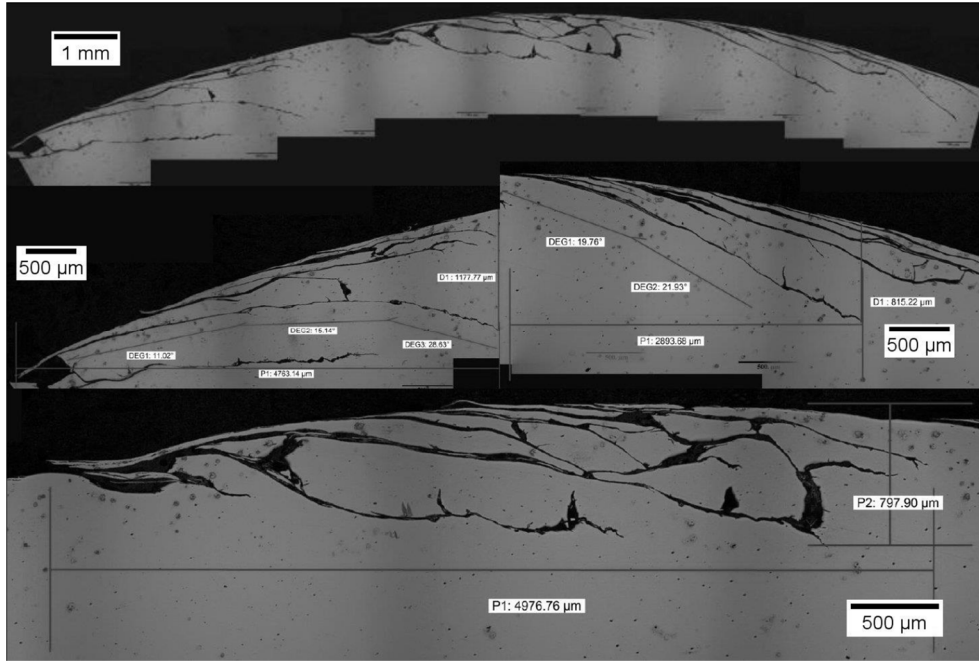


Figure 16: Test 6, 4000 Cycles Dry, 21000 TOR Lubricant (Oil)

After the application of the oil-based TOR lubricant large amounts of surface damage, similar to when water has been applied, was observed (see Figure 10 Sample 6). The subsurface overview (see Figure 16) shows multiple long bifurcated cracks branching both towards the surface and down into the rail specimen. The cracks appear similar to those observed when water was applied. Some cracks follow the surface for quite some distance before turning down into the rail. Located in the centre of the overview is a site where multiple joining cracks have formed breaking the surface at several points. Crack lengths were measured and range from 2900 µm - 4800 µm with the maximum depth ranging from 815 µm - 1200 µm. Crack angles were typically between 20 – 30 degrees with some crack tips turning almost vertical. The zone with multiple joining cracks was measured to be almost 5mm long with a depth of 0.8 mm.

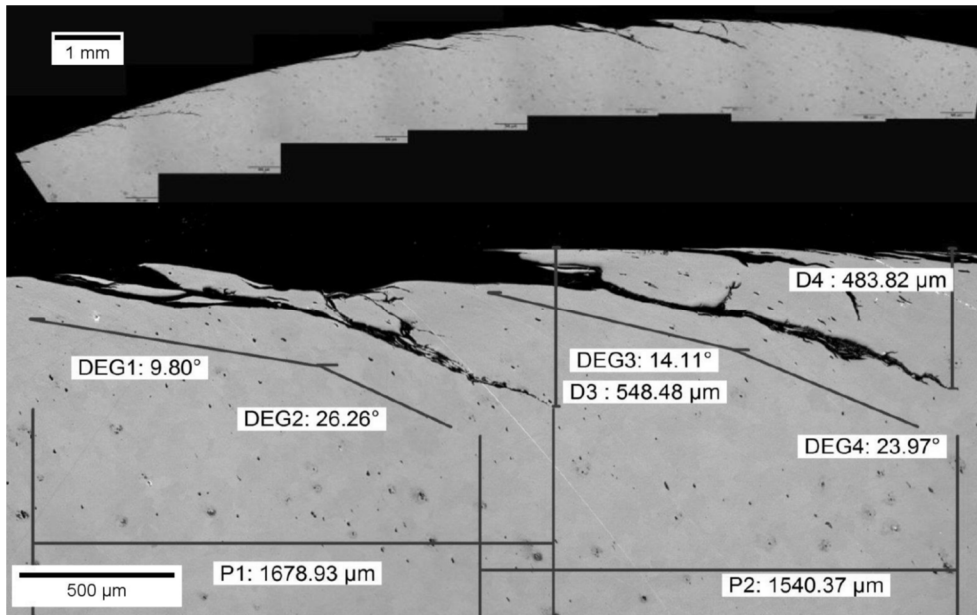


Figure 17: Test 7, 4000 Cycles Dry, 21000 Cycles TOR Lubricant (Grease)

The surface of the R350HT rail specimen after the grease-based TOR lubricant is shown in Figure 10 sample 7. It can be seen that the surface has regions where the damage is minimal; similar to that seen under dry conditions, however, there are areas where surface cracking can be clearly seen along with signs of spalling where large chunks of material have been removed. Looking at the subsurface cross-section overview (see Figure 17) it can be seen that frequent surface breaking cracks are present. These are similar to the gauge face lubricant test for the same depth. Cracks ranged in length from 1540 μm – 1680 μm reaching depths of 550 μm. In contrast to the synthetic oil based product and the gauge face lubricant far less crack branching was seen. Crack angles range from 10- 26 degrees.

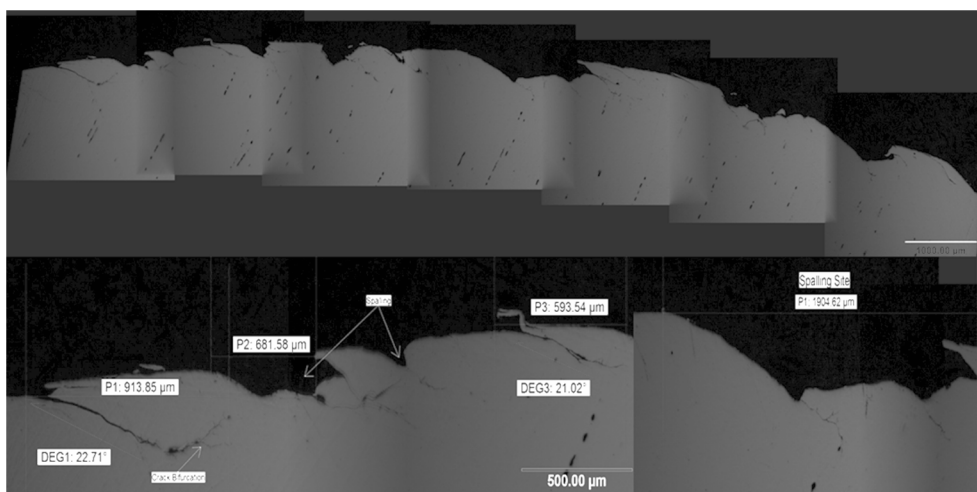


Figure 18: Test 8, 4000 Cycles Dry, 21000 Cycles TOR Hybrid

The TOR hybrid material (an oil-in-water emulsion) provides a stable, but very low (0.02) coefficient of traction. Surface damage is characterised by shallow spalling and pitting (see Figure 10 Sample 8), similar to that of the gauge face lubricant and the grease based TOR lubricant. An 11% reduction in wear as measured by mass loss and compared to the dry baseline is observed. Subsurface investigation (see Figure 18) shows a number of spalling areas, some up to 1.9mm in length. Cracks tend to propagate in the rail material and then diverge often with one branch heading towards the surface leading to spalling. Crack lengths were measured up to 900 μm with depths up to 500. Despite its limited water content this material stayed wet on the disk surface during the whole test.

Table 4 shows a summary of the crack information from all the specimens.

Table 4: Crack Length, Depth, Angle, Distribution

Test	Product	Notes	Max Crack Length (μm)	Max Crack Depth (μm)	Crack Angles (Deg)	Comments
1	n/a	Initial Dry	227 - 522	25 - 70	0 - 17	Infrequent shallow cracks
2	n/a	Full Cycles	383 - 495	35 - 48	0 - 8	Frequent shallow cracks
3	Water	Wet Rail Baseline	944 - 1900	212 - 361	0 - 90	High material removal (flakes)
4	A	TOR FM (Drying)	570 - 686	51 - 90	0 - 18	Frequent Shallow Cracks
5	B	Gauge Face Lubricant	2350 - 2415	1100 - 1232	49 - 90	Localised spalling
6	C	TOR Lubricant (Oil)	2900 - 4800	815 - 1200	20 - 30	High material removal, multiple conjoining cracks
7	D	TOR Lubricant (Grease)	1540 - 1680	483 - 550	10 - 26	Localised spalling
8	E	TOR Hybrid (Non Drying)	593 - 914	250 - 500	20 - 23	Localised spalling

4 DISCUSSION

4.1 Friction, Wear and Cracking Behaviour

The initial baseline test over 4000 cycles provided an average dry coefficient of traction between 0.36 - 0.40, typical of test run under these condition on this test platform. The slight reduction in the coefficient of traction over time is most likely due to temperature generation within the contact. The imparted surface damage is minimal as seen in Figure 10 sample 1. No surface cracks were observed and analysis of the cross section indicated that short shallow cracks of lengths ranging from 250 μm – 500 μm with a depth between 30 μm – 70 μm had developed.

When increasing the number of dry cycles from 4000 to 25000 cycles a rise in surface damage was observed (see Figure 10 sample 2). Although the damage had increased, and

surface cracks were now visible, there were no signs of significant material removal. An increase in crack frequency was observed and the crack depths were slightly lower than seen with just 4000 dry cycles, this is most likely due to a two-fold increase in the wear rate. The increased wear will be removing material from the crack mouth and thus reduce the crack growth rate.

The application of water to the specimens after 4000 dry cycles had a dramatic effect on the mass loss. An increase in wear rate of 1739% compared to the dry case that had undergone the same number of cycles. The application of water reduced the coefficient of traction from 0.46 to 0.2. This is typical of a flooded contact. Lower values may be achieved by reducing the amount of water applied. The surface of the rail disc showed catastrophic damage (see Figure 10 Sample 3). The large cracks evident are consistent with RCF delamination. During the test large chunks of metal were regularly being removed from the rail specimen surfaces through delamination / flaking. Crack frequency, length, and depth increased significantly. Analysis of cross sections cut out of the rail specimen (see Figure 13) revealed long cracks which run parallel to the surface before turning down and propagating into the bulk material. Crack lengths were up to 1900 μm and crack depths up to 361 μm . Bower [15], showed that cyclic shear crack growth (Mode II) was unlikely to occur if the crack face friction (CFF) was greater than 0.2. **CFF could not be measured in the current tests, but in sliding contacts and rolling sliding contacts (as in this work), a steel/steel interface with water present gives a friction coefficient of around 0.2.** This evidence points to hydro-pressurisation or borderline growth under CFF controlled shear as the cause of the crack growth under the application of water.

The application of the water based friction modifier reduced the traction coefficient to 0.12 although it must be stated that it took multiple applications until this stable level was reached (see Figure 4). No data exists pertaining to the amount of product entrained in to the contact patch under real-world applications, it should be understood that the amount used was based on recommendations and kept constant for all products. This allows for this investigation of the product, rather than application rate.

With the TOR friction modifier wear rates were 44% lower than witnessed during dry baseline. The surface of the rail specimen looked similar to the dry baseline tests. Some scratches were visible, but there were no signs of crack accumulation. The effects of the application were minimal on crack propagation. When looking at the subsurface cross sections (Figure 14: Test 4, 4000 Cycles Dry, 21000 Cycles TOR FM cracks are similar in length and depth to the initial 4000 dry cycle case. This shows that it is not causing any acceleration of crack growth and there is no hydro-pressurisation or crack flank lubrication occurring. The wear rate is lower than the 25000 dry cycle test which would suggest that crack truncation is not taking place to the same extent. It can be deduced that the reduced traction creep force had moved the contact into the elastic shakedown regime (for the work hardened rail surface), within which no further crack growth occurs.

The gauge face lubricant reduced the coefficient of traction to 0.06 – 0.07 and it remained constant for the test duration (see Figure 5). This traction is as expected for lubricants. Application also reduced wear over the dry baseline case by 73% as measured by mass loss. However, visual inspection of the disc surface showed regions of surface cracking and the initiation of delamination. This was consistent with testing performed in the development of the Network Rail lubricant performance standard [1]. The cross section overview of the rail

material contains several long cracks propagating down deep into the material (see Figure 16). The cracks appear wider than witnessed in the previous tests with the application of water and TOR FM. Cracks varied in length from 2350 μm – 2415 μm which is slightly shorter than that witnessed with the application of water. The cracks were wide and retained a fairly constant crack angle with no crack branching. With an increased viscosity over water and a lower coefficient of traction, it could be hypothesised that crack growth and spalling is driven by crack face lubrication as opposed to hydro-pressurisation.

The application of a synthetic oil based TOR lubricant also reduced the coefficient of traction to between 0.06 – 0.07, as expected for a lubricant. There was an increase that remained constant to the end of the test starting at about 15000 cycles (see Figure 6). This increase was probably caused by the large degradation of the specimen surfaces, the collapse of the lubricating film and the entrainment of wear particles leading to three-body abrasion. The application of the oil based product increased the wear mainly due to crack delamination and spalling by a 1248%. The disc surface was similar in appearance to that witnessed with water, showing large amounts of deformation and delamination (see Figure 10). There were numerous cracks running for a long distance parallel to the surface before propagating down into the bulk material at a constant angle. The low viscosity and low coefficient of traction of the TOR lubricant would suggest that accelerated crack growth may occur due to a combination of both hydro-pressurisation owing to the similarities with water (shallow cracks and delamination) and crack flack lubrication (increased spalling) as seen with the gauge face lubricant.

Similar to the oil-based TOR lubricant and the gauge face lubricant, the grease based TOR lubricant displays a reduced traction coefficient between 0.06 – 0.07. There a negligible reduction of 0.05% in wear of the rail material over the dry baseline measurement, although spalling of the surface had occurred. The damage is less than seen with the application of water and the oil based TOR lubricant, it was found to result in a worse effect than the gauge face lubricant. Crack length and depth are generally smaller than observed with the gauge face lubricant but display similar characteristics with respect to crack angle and thickness. This is most likely due to the similarities in traction coefficient and product viscosity.

The TOR hybrid material which is ostensibly an emulsion of oil and water provides a very low coefficient of traction (0.02). Similar effects have been reported in previous studies investigating the effect of oil and water mixtures in the wheel-rail contact [16], recent field trials on a TOR hybrid material have also reported that the achievable COF is strongly dependent on the material application rate. Consequently, a slight over-application can result in low adhesion leading to loss in braking performance [7]. Analysis of the specimen cross-section would suggest similar crack characteristics (orientation, bifurcation and spalling) to that of a gauge face lubricant. With that in mind it would appear that the lubricant in the water is driving crack propagation, however the characteristics are vastly different from that of an oil-based TOR Lubricant.

4.2 Product Influence on RCF

In all cases, except that of the TOR friction modifier, it can be seen that the introduction of a material increases the surface damage. A similar increase in the wear rate is not always observed, such as in the cases of gauge face lubricants, grease-based TOR lubricants and the

TOR hybrid material. In these cases spalling is the main contributor to material loss, it is most likely that spalling occurs during the initial application of these materials after which little further interaction with existing cracks occurs. For the case of friction modifier, the rail exhibited a similar extent of surface damage to that of the dry baseline case from far fewer test cycles.

A ranking of the product’s effect on crack propagation is shown in Figure 19.

TOR Friction Modifier	Stable / No Accelerated Crack Growth. Reduce Rail Wear 44%
Gauge Face Lubricant TOR Hybrid (Oil + Water) TOR Lubricant (High Viscosity Grease)	Initial Spalling with Application, Slight Further Crack Interaction. Reduced Rail Wear 0.06 – 72%
TOR Lubricant (Low Viscosity Oil) Water (Flooded Contact)	Accelerated Crack Growth. Surface Delamination and Increased Material Loss up to 1740%

Figure 19: Ranking of product effect on crack propagation

Assessment of the coefficient of traction for all the materials tested (see

Table 2) with consideration to the properties of the rail material and contact pressures used reveals that the stress state of the rail material lies within the elastic/plastic region on a shakedown plot, meaning that when the materials are constantly applied to undamaged rail material RCF would not develop, this certainly is consistent with the work of Stock et al. [2] where the application of a friction modifier was tested in a full scale rig on new rail and after 100,000 cycles no signs of RCF appeared.

The mechanism of crack interaction under product application is not determined by this testing. It could be caused by crack pressurisation or crack face lubrication or a combination of both [15, 18]. However, the products must be able to enter the cracks to cause accelerated crack growth. Bower [15], showed that cyclic shear crack growth (Mode II) was unlikely to occur if the crack face friction was greater than 0.2.

With respect to the coefficient of traction measured during material application (see

Table 2) it can be seen that water has a traction coefficient around 0.2. With water being on the cusp of Bower's limit it would suggest that crack pressurisation is more likely. All other products result in a traction coefficient below Bower's limit of 0.2, in fact the TOR hybrid (Oil-water emulsion) has a coefficient of traction of 0.02 well below that expected of a gauge face lubricant. This would suggest that these products if entrained into a crack will lubricate the crack flanks leading to accelerated crack growth but, does not discount crack tip pressurisation.

For a fluid to cause accelerated crack growth by pressurisation it must be entrained or forced into the crack mouth. FEA modelling [19] suggests that under normal rail operational speeds, crack mouth opening is too rapid to allow a fluid to be entrained into the crack. This, however, is occurring during the twin-disc testing, this may be due to the line contact geometry.

The FEA work further suggests the mechanism for a fluid on the rail head to be entrained into the crack is by means of capillary action. If this is the case, viscosity of the fluid must play a part in the fluids susceptibility to be entrained in to a crack.

Although viscosity measurements were not performed on the products tested in this work, it is clear from the qualitative classification that water has the lowest viscosity, followed by the synthetic oil-based TOR lubricant, the TOR Hybrid then the friction modifier. The gauge face lubricant and the grease based TOR lubricant products have the highest viscosity.

Interestingly, of the materials tested the two low viscosity substances, water and the oil TOR lubricant, caused the most damage. With the exception of the TOR friction modifier, which resulted in no accelerated crack growth, the least impact was witnessed with the application of the gauge face lubricant and the grease-based TOR lubricant, both of which share a similar viscosity.

In the case of the friction modifier the low amount of surface damage can be explained by the rapid evaporation of the water content under the contact conditions which leaves behind a film of solid particulate that either does not enter the crack mouth, or if it does, it does not penetrate deep enough to lubricate a sufficient portion of the crack flanks. When in its liquid form such materials may be susceptible to pressurisation of existing cracks., However, based on the results presented in this paper, this liquid-state time period of the FM appears to be sufficiently short so that it does not pose a significant risk of accelerated crack growth. It is planned to investigate these crack growth possibilities in extension to the current work using models developed subsequent to Bower's work [20, 21], allowing investigation of the interaction between surface and crack face friction which can be varied independently between modelling runs to represent rail head treatments which enter (or do not enter) surface breaking cracks.

4.3 Field Studies

So far no extended field studies are available on this topic. However, there is some anecdotal heavy haul experience indicating that spalling can occur in the vicinity of wayside application bars (especially for GF lubrication) if pre-existing cracks are present on the rail surface. In general, the crack layout of typical RCF damage in curves has a much complex geometry compared to damage forming at the disc surface at the SUROS. Such a complex 3D

geometry of a typical gauge corner crack will easily allow any liquid material to escape from the crack tip during loading / over-rolling. However, especially in transition curves a crack geometry can be found on the rail surface that is close to the crack geometry of a typical twin-disc experiment. This is in correspondence with the above mentioned anecdotal evidence of liquid-crack interaction.

Furthermore, factors like the amount of TOR product present on the rail surface, the used rail grade (RCF resistance) and the grinding cycles as well as quality of grinding (remaining surface cracks) will have an impact on liquid crack interaction under operational conditions. Besides this spalling of the rail surface, can also occur due to other reasons than liquid crack interaction.

Consequently, it can be difficult to directly correlate spalling with liquid-crack interaction without conducting a dedicated and well controlled track test/examination.

5 Recommendation for future work

In order to assess the danger/likelihood of liquid crack interaction under real track conditions a dedicated test set-up is recommended that tries to eliminate as many as possible other influencing factors on the development of spalling. As such a track test might be difficult to control and of relatively long duration (months or years) an intermediate step seems to be appropriate. A full scale test set-up (as used in [2]) might be helpful to better determine the necessary parameters to cause accelerated crack growth and spalling by liquid crack interaction under real geometrical contact and loading conditions. The output of such a well planned and executed test will then hopefully help to reduce the scope and length of a possible track test.

6 CONCLUSIONS

Laboratory testing was performed to assess the impact of the application various friction management material on rail with pre-existing RCF cracks. The methods used to initiate RCF were based on existing protocols for the assessment of different rail material. Product application was the same for all products allowing for direct comparison.

Results suggest that the application of a low viscosity, low coefficient of traction product such as “oil” based TOR lubricant to a rail that already exhibits damage is not recommended as accelerated crack growth is a possibility. Materials such as gauge face lubricants, grease-based high viscosity TOR lubricants and TOR hybrid (oil-water emulsion) may also interact with existing cracks leading to spalling. Once the initial cracks have spalled out, the material interaction with new cracks appears limited.

Out of the products tested only the friction modifier resulted in a reduction in wear coupled with no acceleration of surface damage and cracking.

Generally, the application of non-drying fluid based materials to a rail surface with pre-existing RCF damage will with a high likelihood serve to further deteriorate the state of the rail by causing accelerated crack growth and/or spalling. Only in the case of the water based, drying friction modifier the carrier fluid can evaporated quickly enough under the contact temperature resulting in only dry FM particles to be present between wheel and rail that do

not interact with pre-existing cracks. Unlike a drying FM, the oil and grease based products remain in a liquid state under wheel-rail contact pressure and temperature conditions and can result in severe liquid-crack interaction.

A firm conclusion as to the mechanism for this accelerated crack growth has not been reached. Both fluid pressurisation and crack flank lubrication are thought to contribute dependent on the material characteristics.

Further studies are required in this area namely to identify the mechanism of accelerated crack growth and parameters to govern material entrainment into cracks. Additional work utilising full-scale wheel-rail testing facilities and field trials are recommended.

7 REFERENCES

- [1] R. Stock, D. Eadie, and K. Oldknow. Rail grade selection and friction management: a combined approach for optimising rail-wheel contact - rail grade selection and friction management: a combined approach for optimising rail-wheel contact. *Ironmaking & Steelmaking*, 40:108 – 114, 2013.
- [2] R. Stock, D.T. Eadie, D. Elvidge, and K. Oldknow. Influencing rolling contact fatigue through top of rail friction modifier application - a full scale wheel-rail test rig study. *Wear*, 271:134–142, 2011.
- [3] A. R. S. Ponter, A. D. Hearle, and K. L. Johnson. Application of the kinematical shakedown theorem to rolling and sliding point contacts. *Wear*, 33:339–362, 1985.
- [4] K. Dang Van and M. H. Maitournam. Rolling contact in railways: modeling, simulation and damage prediction. *Fatigue and Fracture of Engineering Materials and Structures*, 26:939–948, 2003.
- [5] S. L. Grassie and J. Kalousek. Rolling contact fatigue of rails: characteristic, causes and treatment. In *6th International Heavy Haul Association Conference Proceedings in Cape Town, South Africa*, pages 381–404, 1997.
- [6] G. Trummer, K. Six, C. Marte, P. Dietmaier, and C. Sommitsch. An approximate model to predict near-surface ratcheting of rails under high traction coefficients. *Wear*, 314 Issue 1-2:28–35, 2014.
- [7] S. L. Grassie. Studs and squats: The evolving story. *Wear*, page In Press (Available Online), 2016.
- [8] R. Stock, L. Stanlake, C. Hardwick, M. Yu, and D. T. Eadie and R. Lewis. Material concepts for top of rail friction management - classification, characterization and application. *Wear*, In Press (Available Online), 2016.
- [9] D. I. Fletcher and J. H. Beynon. Development of a machine for closely controlled rolling contact fatigue and wear testing under high stress. *Journal of Testing and Evaluation*, 28:267–275, 2000.
- [10] E. E. Magel and Y. Liu. Some aspects of the wheel/rail interface. *Wear*, 314:132-139, 2014.

- [11] J. H. Beynon and D. I. Fletcher. The influence of lubricant type on rolling contact fatigue of pearlitic rail steel. *Proceedings of the 25th Leeds-Lyon Symposium on Tribology*, pages 299–310, 1999.
- [12] W. R. Tyfour, J. H. Beynon, and A. Kapoor. Deterioration of rolling contact fatigue life of pearlitic rail steel due to dry-wet rolling-sliding line contact. *Wear*, 197:255–265, 1996.
- [13] B. Paulsson and A. Ekberg. Innotrack - concluding technical report. Technical report, International Union of Railways (UIC), 2010.
- [14] Network Rail. Curve lubricants, 2012.
- [15] A. F. Bower. The influence of crack face friction and trapped fluid on rolling contact fatigue cracks. *ASME Journal of Tribology*, 110:704–711, 1988.
- [16] T. Hilton, T. Armitage, R. Lewis, and E. A. Gallardo-Hernandez. Effect of oil and water mixtures on adhesion in the wheel/rail contact. *Proceedings of the Institution of Mechanical Engineers Part F, Journal of Rail and Rapid Transit*, 223:275–283, 2009.
- [17] J. Lundberg, M. Rantatalo, C. Wanhainen, and J. Casselgren. Measurements of friction coefficients between rails lubricated with a friction modifier and the wheels of an iore locomotive during real working conditions. *Wear*, 324-325:109–117, 2015.
- [18] I. Kudish and K. W. Burris. Modeling of surface and subsurface crack behavior under contact load in the presence of lubricant. *International Journal of Fracture*, 125:125–147, 2004.
- [19] S. Bogdanski. Liquid solid interaction in rolling contact fatigue cracks. *Proceedings of the 6th International Conference on Contact Mechanics and Wear of Rail/Wheel Systems (CM2003)*, pages 93–98, 2003.
- [20] D. I. Fletcher and A. Kapoor. A simple method of stress intensity factor calculation for inclined surface-breaking cracks with crack face friction under contact loading. *Proceedings of the Institution of Mechanical Engineers Part J, Journal of Engineering Tribology*, 213:481–486, 1999.
- [21] D. I. Fletcher and J. H. Beynon. A simple method of stress intensity factor calculation for inclined fluid-filled surface- breaking cracks under contact loading. *Proceedings of the Institution of Mechanical Engineers Part J, Journal of Engineering Tribology*, 213:299–304, 1999.